APR 27 1998

UB-PUB-EPPG-PHYS-38

BUCHAREST UNIVERSITY

EXPERIMENTAL PARTICLE PHYSICS GROUP

UBPub .EPPG/PHYS 38
March 1998

Fermilab Library
0 1160 0075644 7

INFLUENCE OF THE GEOMETRICAL LAYOUT OF THE SILICON MICROSTRIP DETECTORS ON ELECTRICAL CHARACTERISTICS

T. ANGELESCU, A. MIHUL
UNIVERSITY OF BUCHAREST, ROMANIA

O. MILITARU, M. PENTIA
NATIONAL INSTITUTE OF PHYSICS AND NUCLEAR ENGINEERING, ROMANIA

KEYWORDS: SILICON MICROSTRIPS, EDGE EFFECTS, BREAKDOWN

To be presented at MIXDES'98, The 5-th International Conference on Mixed Design of Integrated Circuits and Systems. Lödz Poland 18-20 Juin 1998

Abstract

In the present particle physics experiments, high resistivity silicon sensors are often used. In tracking detectors for the LHC accelerator at CERN this type of detectors has to fulfill special requirements due to high radiation environment due the proton-proton collision. Because of the radiation damages in n-type silicon bulk, high bias voltage has to be applied in order to obtain efficient charge collection. The rising of the bias voltage is limited by the breakdown process appearance.

The geometrical characteristics of the active microstrips area are essential for the detection performances. Important geometrical parameters as microstrips and readout pitch, distance between p+ multiguardrings, between the last guardring and sensors border, influence the electrical parameters as operating bias voltage at which breakdown process appears. This effect is crucial in time stability of the experiment. Computer simulation and theoretical results in study of the edge effects are detailed and conclusions about some geometrical parameters are presented.

RETURN TO FERMILAB LIBRARY

Aims

The UBPub. EPPG/Phys series of paper aims is in the first place to reflect the activities of the Experimental Particle Physics Group (EPPG) of the Bucharest University and of related groups. The publications report on research and progress in the field of Physics, Engineering and Instrumentation

Publications of outside groups are strongly encouraged.

The material presented for multiplication is usually accepted only after positive recommendations of at least two independent specialist referees.

Publisher

Experimental Particle Physics Group
Bucharest University Faculty of Physics
Bucharest Magurele POBox Mg 12

Board of Editors.

Prof. Alexandru Mihul E-mail Alexandru.Mihul@cern.ch
Prof. Tatiana Angelescu E-mail angt@scut.fizica.unibuc.ro
Prof. Ionut Lazanu E-mail ilaz@scut.fizica.unibuc.ro
Dr. Gheorghe Stratan E-mail stratan@roifa.ifa.ro

Disclaimer

Neither the Bucharest University nor the Board of Editors makes any warranty, expressed or implied, or assumes any legal liability or responsibility for the accuracy, completeness, or usefulness of any information, apparatus product, or process disclosed, or represents that its use would not infringe privately owned rights. References herein to any specific, commercial product, process, or service by trade name, trademark, manufacturer, or otherwise, do not necessarily constitute or imply its endorsement, recommendation, or favouring by the Bucharest University.
The views expressed in the publications do not necessary represent those of the Bucharest University or of the board of editors

Dissemination

Reprinting and further dissemination is permitted with proper acknowledgements.

INTRODUCTION

The CERN Large Hadron Collider (LHC) will achieve unprecedented energies and luminosity in the search for new particles and tests of actual theories. The very intense radiation level resulting from such energy and luminosity both from neutron emission and high charged particle flux will create many problems to any detection system at LHC.
One of the experiments proposed at CERN is the Compact Muon Solenoid (CMS) project. The CMS collaboration proposed a detector for proton-proton collider at LHC, guiding the detector optimization by physics issues such as the Higgs boson and supersymmetry searches. The experiment will operate at the highest possible luminosity where these searches will take place.
The requirement for a compact design led to the use of a superconducting solenoid with large radius (about 3 m), generating a magnetic field of about 4T. The large radius allows the full calorimetry to be located inside the solenoid.
The variety of the final states for proton-proton collision led to the basic design considerations as follows:
-a sensible electromagnetic calorimetry for electron and photon identification and measurements, in addition to effective hadron calorimetry;
-an efficient lepton tracking and momentum measurements at high luminosity;
-a precision muon measurements;

For such purposes silicon detectors have been used for many years in a variety of applications. In particular, in HEP experiments they offer high detection efficiency, low mass, high speed response and competitive cost. Now that processing technology has improved, very high position resolution can be achieved and two dimensional readout is possible with double-sided and pixel detectors.
Constructing the CMS tracking detector in silicon pixel, single-sided and double-sided silicon strips and MSGC detectors layers optimizes the cost/performance ratio. Because of the high magnetic field at CMS, a good momentum resolution is achievable with only a few, high precision, detection planes. In the same time, the good track finding capability sets a lower limit on the number of detection planes.

CENTRAL TRACKING

The central tracking system will play a major part in all physics searches. The design goal of the central tracking system for CMS experiment is to reconstruct isolated high p_T tracks with an efficiency of better than 95% and high p_T tracks within jets with an efficiency of better than 90% over the rapidity range $|\eta| < 2.6$.
Due to the primary hadron-hadron interactions, the detectors will be exposed to high radiation level from charged particles, gammas and neutrons. It is expected that, after 10 years of running, depending on the distance from the beam line, the silicon sensors will acquire an overall integrated fluence of about $(1+3)\times10^{14}$ charged particles/cm^2. In particular, for silicon microstrips layers, such high levels of radiation will be the source of many changes, regarding operating parameters (ref.[1]).
The n-type silicon bulk detectors undergo type inversion, the silicon becoming effectively p-type. Therefore, the required bias voltage for full depletion will increase and other important detector parameters as interstrip capacitance will be affected, as well.
In these conditions, overdepletion is needed to fully collect the charge by increasing the charge carrier velocity and to lower the noise by reducing the interstrip capacitance. The rising of the bias voltage is limited by the beginning of the breakdown process which depends on the electric field in different regions of the sensors. In order to ensure a large operating domain of the bias voltage for the time stability of the experiment, the study of the breakdown process is very important in detectors design (ref. [2],[3]).

OPERATION OF DETECTORS

The most used design of single-sided silicon microstrips sensors consists in a succession of many p+ strips diodes on a lightly n doped silicon bulk.
The detector is operated with reverse bias, in order to achieve a fully depleted substrate. When a charge particle passes through the detector, electron-holes pairs are created along the particle track. These are separated before they can recombine by the electric field in the silicon bulk and induce signals at the electrodes. The leakage current together with the collection of holes or electrons pulse appears as a current, the integration of which equals the total charge deposited in the silicon. The coordinate of the particle is taken as the weighted strip coordinate with the large signal, and the best possible resolution is given by:
$\sigma = (\text{pitch})/\sqrt{12}$. The resolution might be improved by reducing the strip pitch (the distance between strips), so obtaining a more efficient charge spread between strips. Recent in microstrips designs with 25 μm pitch good charge sharing was obtained.
The silicon microstrips detectors operate with significant overbias, where the applied voltage is much higher than the full depletion voltage. The overbias increases the bulk electric field, proportional to the applied voltage. The limit of the bias voltage is determined by the breakdown characteristics of the detector.

GEOMETRICAL CHARACTERISTICS

The geometrical characteristics of the active microstrips area are very important for the detection performances. Essential geometrical parameters as microstrips and readout pitch, distance between p+ guardrings, distance

between the last guardring and sensors border influence the electrical parameters as the interstrip capacitance and the operating bias voltage at which breakdown process appears. In several HEP projects, multiguardrings implants were proposed, in order to diminish the electric field around the microstrips area (ref. [4],[11],[12],[13]).

In multiguardrings configuration it has to be taken into account that:
-the reserved space is limited, this zone being ineffective from the point of view of particles detection;
-in order to prevent the bulk and surface leakage current rising due to mechanical cuts from the wafers border, each sensor edge has n+ implants on both surfaces. For a large range of bias voltage, the both surfaces remains at the same potential, and the electrons from marginal damaged zone are kept out from the detection area. On the other hand, the distance that should be left with respect to sensor border limits the number of multiguardrings, considering that the electric field at the last guardring region is much influenced by the vicinity of the marginal n+ implant.
Another fact that we took into account is the presence of the positive charge trapped in the grown oxide over the silicon wafer. This charge induces an electron accumulation layer under the oxide that significantly influences the breakdown voltage (V_{BD}).

COMPUTER SIMULATION AND THEORETICAL RESULTS

In this study we used computer simulations and theoretical computations to enable the design of the region of multiguardrings and sensors border in silicon full-size detectors. The work consists in studying the right configuration between the last p+ guardring and the sensor border n+ implanted, in order to obtain the highest breakdown threshold for the bias voltage. The design under investigation is presented in fig. 1.

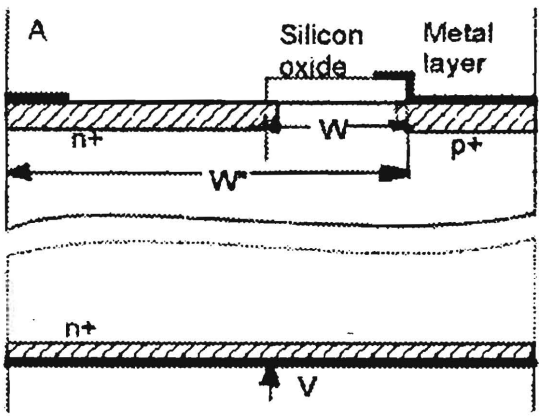

Fig.1 Cross section of the studied region

The figure represents the configuration of the last p+ guardring (right side) and the beginning of the n+ wall (left side) at the end of a single-sided, light doped n-type sensor. The back side is n+ implanted all over, covered by a metal layer. A metal layer is over the p+ implant also, overlapping the silicon oxide with 5 microns. W and W* are the distances between p+ and n+ implants and respective, between p+ and sensor mechanical cut, represented by A line. The B side is toward the inner region of the sensor, where the microstrips active area is.
During the functioning of the detector, bias voltage is applied on the ohmic side, keeping the upper side p+ implant at ground.
We used computer simulation for the structure represented in Fig.1, to obtain the potential and the electric field distribution and currents characteristics at different values of bias voltage applied to the p^+ n junction.
Breakdown voltage was determined for different W and W* values configurations. It was expected that the region of maximum electric field to be situated at the p+ implant corner and to be influenced by two main factors:
-the presence of the n+ implant in vicinity and,
-the electron accumulation layer under the silicon oxide.
The software package used for simulations were ISE (Integrated Systems Engineering AG-ISE) developed at ETH Zentrum, ETH Zurich-Switzerland, which models semiconductor technology, devices and systems (ref. [7]). The program models semiconductor devices, calculating static and dynamic parameters in the conditions supplied by user. From the package, $MDRAW_{-ISE}$ was used as mesh generator. As geometrical input values, some data for implant shapes from specialized literature were taken. We used: p+ implant depth of 1.2 μm, the upper side n+ implant depth of 1 μm, the ohmic side n+ implant depth of 1.8 μm. For all implants, lateral diffusion was of about 0.7 μm. Boron atoms were used for p^+ implants and Phosphor atoms for n^+ implants. In $DESSIS_{-ISE}$ main program two general models were used:

-the *drift diffusion* model; which solves Poisson equation together with electron and hole current continuity equations, and

-the *thermodynamic* model; which simulates the effects of self-heating on the temperature distribution and the effects of the non-uniform temperature distribution on the electrical characteristics. Thus the temperature equation was solved. Such a model extends the drift-diffusion approach taking into account electrothermal effects, under the assumption that the charge carriers are in thermal equilibrium with the lattice.

In both cases, different particular physical models were used, namely: the generation-recombination with terms for avalanche process and Shockley-Read-Hall recombination (which depends on doping concentration), Auger recombination, tunneling recombination (for high electric fields) and surface recombination.
We also took into account the mobility dependence on

doping and electric field intensity, in surface layers of the devices. Parameters used in all simulation programs were surface recombination velocity of 5cm/sec, carriers lifetime of 10^{-2} sec.
The generated grid by MDRAW-ISE was at the upper limit, i.e. a mesh of about 10000 points was used. With this grid the program DESSIS-ISE occupied approx. 28 MB of RAM on the HEWLETT PACKARD 10.20 station. About 20 hours were needed for these calculations until the breakdown voltage was reached.
The I-V characteristics with the data from current data file generated by DESSIS-ISE were visualized with the SEPP program from the same package.
Using PICASSO-ISE program, to visualize the calculated parameters, the regions of maximum electric field and it absolute value could be approximated.

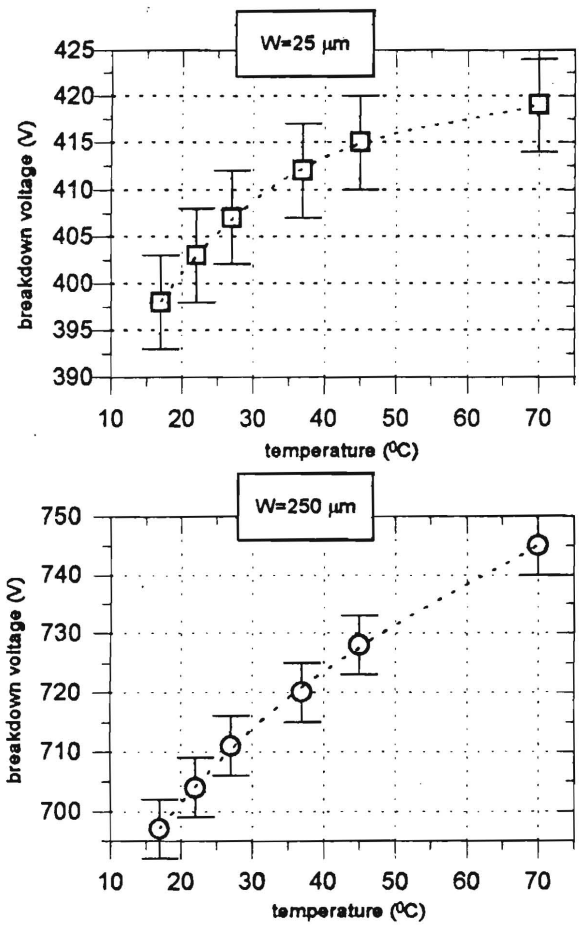

Fig.2 Temperature dependence of the breakdown voltage for W=25 and 250 microns.

Simulation of I-V characteristics for W of 15, 25, 75, 100, 150 and 250 microns were done.
Structures with W of 25 and 250 microns were simulated, also at different values of external temperature, and I-V characteristics were obtained. Considering the breakdown voltage in each case, it was possible to define a calibration curve of the breakdown voltage versus temperature (fig.2). These plots might be used to correct the experimental data taken at different external temperature. In all graphics, the error of the breakdown voltage values is ± 10V, because of the "soft" breakdown obtained in simulations.

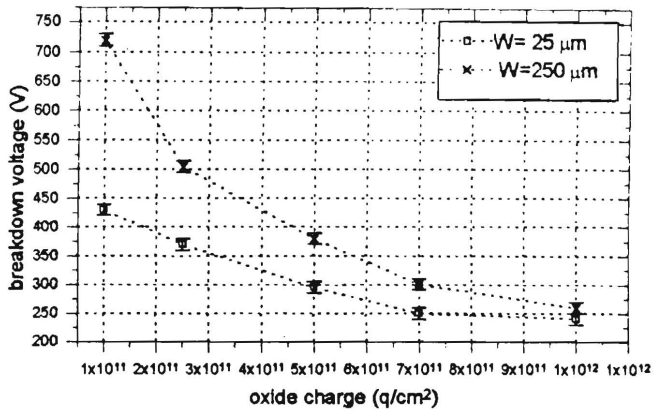

Fig. 3 The dependence between breakdown voltage and silicon oxide charge, for $6x10^{11}$ atoms/cm^3 n-type bulk doping concentration.

For the corrections related to the oxide charge, considering that its presence has an important influence on the electric field at the diode edge, simulations were made for the same layouts at five different values of oxide charge. The results are presented in fig.3, for $6x10^{11}$ atoms/cm^3 bulk doping concentration at 300^0 K temperature. The assumed oxide charge density was of $1x10^{11}$, $2.5x10^{11}$, $5x10^{11}$, $7x10^{11}$ and $1x10^{12}$ q/cm^2. One can observe the high influence of the accumulation layer of electrons at the interface between Si and SiO_2, on the values of electric field at the diode junction and implicit on the breakdown bias voltage.

For comparison, also theoretical computations were made, for the punch-through and avalanche multiplication phenomenon. Two types of computing were done:

-the *punch-through* breakdown voltage for a diode which consists of three zones p+, n, n+. The breakdown voltage of a punch-through diode V_{PT} was calculated following the analysis made in ref.[5]:

$$V_{PT} = 4010 N_A^{1/8} W - \frac{q N_A W^2}{2\varepsilon_s} \qquad (1)$$

where N_A is the bulk doping concentration (atoms/cm^3), W is the distance between p+ and n+ implants, ε_s is the relative electrical permitivity; and

-the *avalanche* breakdown voltage of a cylindrical

junction V_{BDcyl}, where the implant edge effects were considered. In this case, the electric field increases due to geometrical shape of the p+ implant, diminishing the breakdown voltage of device below the ideal value of a semi-infinite junction. The breakdown voltage for a cylindrical junction normalized to the breakdown voltage of the parallel plane case, V_{BDpp} might be obtained, as an expression that is independent of the specific background doping level, (ref.[5]), as follows:

$$\frac{V_{BDcyl}}{V_{BDpp}} = \left\{ \frac{1}{2}\left[\left(\frac{r_j}{W_{pp}}\right)^2 + 2\left(\frac{r_j}{W_{pp}}\right)^{6/7}\right] \ln\left[1 + 2\left(\frac{W_{pp}}{r_j}\right)^{8/7}\right] - \left(\frac{r_j}{W_{pp}}\right)^{6/7} \right\} \quad (2)$$

Where W_{pp} is the depletion layer width at breakdown for the parallel-plane junction and r_j is the curvature radius of the p+ implant edge (see 3.18 from ref.[5]).

A comparison between theoretical and simulation results are made in fig.4. The punch-through breakdown voltage for three values of bulk doping concentration are presented, calculated with formula (1), together with cylindrical shape junction breakdown voltage for different implant radius, calculated with formula (2). The computer simulation were made for structure with $1x10^{12}$ atoms/cm^3 bulk doping concentration, and two values of silicon oxide charge and p+ implant 1.2 microns corner radius.

This figure could be interpreted as an indication that the breakdown process, for structures with W smaller than 100-150 microns, initiates from a punch-through phenomenon, while for higher values an avalanche process prevails (this value differs with bulk doping concentration). This can be observed from the similar shape of the simulation data and theoretical previsions (plain lines) in the two different W domains. The simulation values for layouts are different with respect to the theoretical ones. This happen mainly because of the presence of the 5 microns of equipotential field plates which rise the breakdown voltage and the electron layer at the interface between Si and SiO_2, modifying the breakdown voltage values in opposite manner. The presence of the field plate and electron accumulation layer of the simulated sensors, were not taken into account in formula (1) and (2). The influence of these two factors might be similar as if the p+ implant edge would have a larger curvature consequently having a higher breakdown voltage.

Therefore, when fitting the simulation data with formula (2) an equivalent parameter r_j' might be obtained, representing the new radius of curvature for the isosurface of the electric field at the corner of the p+ implant. It takes into account the influence of both the field plate and the presence of the electrons accumulation layer.

We studied also, using simulated I-V characteristics, the breakdown voltage values with respect to the distance between the p+ implant and the mechanical cut of the wafer W*. This was needed to find the optimum width of the upper side n+ implant at which the mechanical cut did not influence the electrical functioning parameters. It is expected that, beginning with a certain distance, the cut should not have any influence on the diode breakdown voltage. Simulations were made before and after cut, for W*=250.

Without cut, the border was enough far not to influence the electric parameters. The sensor border cut was simulated with a silicon oxide layer along the line A (see fig.1), with the interface condition for an electron accumulation layer under the oxide, which might be generated by two factors:

-the free electrons from the damaged crystal along the mechanical cut,

-the presence of the silicon oxide with positive trapped charge during the growth.

In simulated I-V characteristics, up to 250V bias voltage, currents on diode on the constant region were different in the two cases, i.e the current for the cutted structure is aprox. 5 time higher then the structure without cut. In the same time, the electric field calculated at the left corner of the p+ implant is lower in the case of cutted structure with respect to the structure without cut. This might be explained considering that the full depletion region extends laterally and reach the damaged region from border. In this situation a high amount of free electrons is collected rising the current at the electrods and lowering the electric field. Even if the breakdown voltage after cut is higher, the charge carrier current rising is not negligible, and might influence the sensor performances.

The simulated breakdown voltage for different W* values are presented in fig. 5. It might be concluded that after W*=400 μm, the values are not influenced by the distance, meaning that probably the damaged region is far enough not be to reached by the full depletion zone.

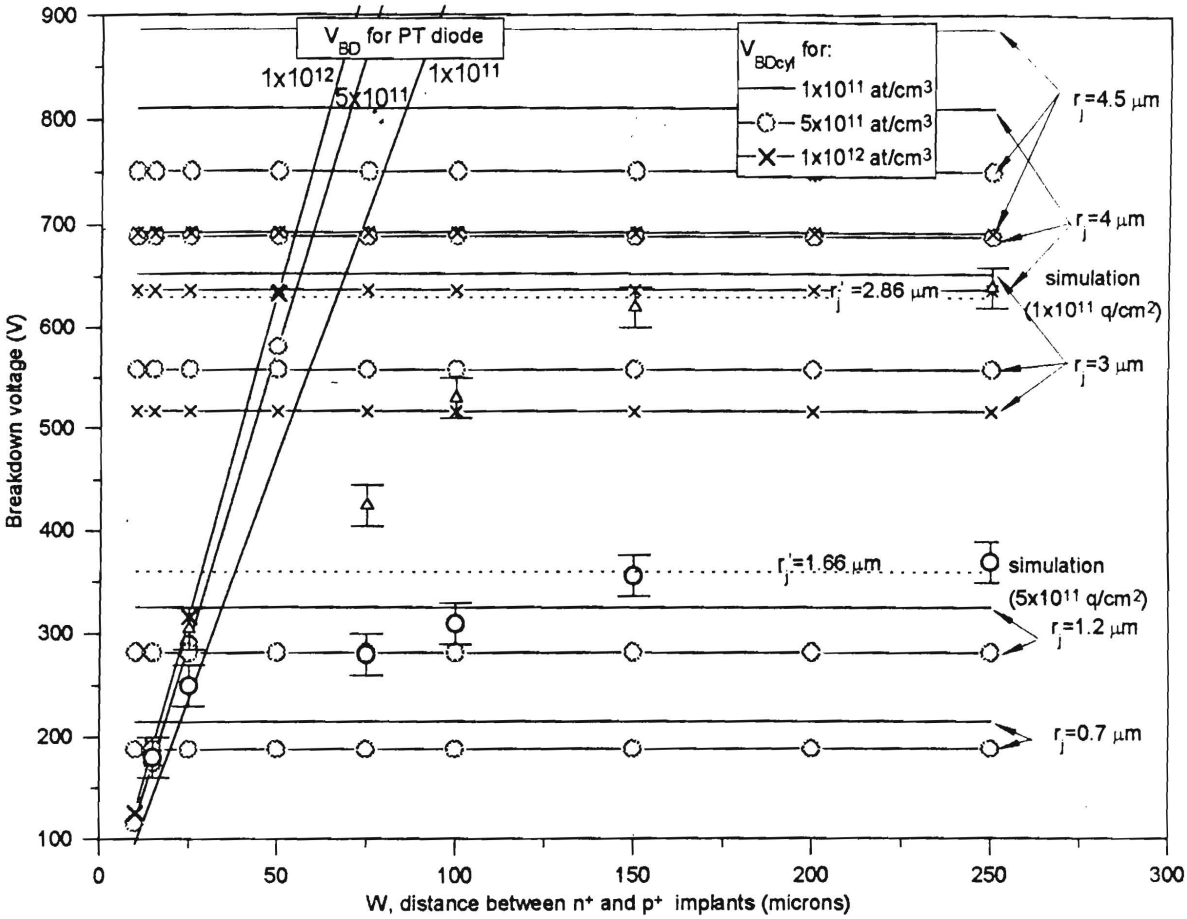

Fig. 4 Theoretical results of the breakdown voltage for punch-through diodes (oblic lines) and cylindrical junction diodes (horizontal lines, for different values of p+ implant curvature r_j) for $1x10^{11}$, $5x10^{11}$ and $1x10^{12}$ atoms/cm^3 bulk doping concentration, represented with plain lines. The simulation data are presented by points with error bars (± 20 V) for $1x10^{12}$ bulk doping concentration for two values of oxide charge. The dot lines are the V_{BD} fitting of the simulation results for the cylindrical junction domain, from which we calculated the equivalent parameter r_j' (see text).

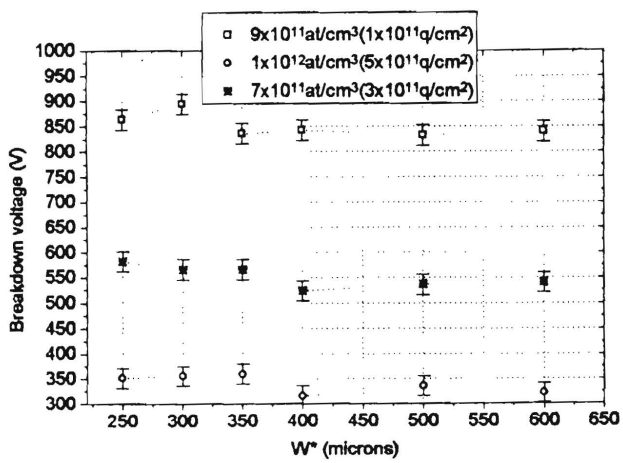

Fig. 5 Simulated breakdown voltage values for different bulk doping concentrations (at/cm^3) and oxide charge (in brackets, q/cm^2) versus the distance between p+ implant and sensor cut.

CONCLUSIONS

The comparison of computed and simulation results reveals that for small distances between p+ and n+ implants the punch-through is the main process that appear while for higher distances avalanche multiplication prevails. The use of the n+ at the sensor edge is necessary to protect the active area from the outside electrons currents. This should be no closer that 100-150 microns (this value slightly depends of the bulk doping concentration). At this point, there is an agreement between simulated and computed data. It might be concluded that, roughly speaking, after 150 microns, the influence of n+ implant on the breakdown voltage value of the diode is very small.

The presence of the outward field plates over the p+ implant is benefic, because compensates the damaging influence of the electron accumulation layer and the result is a higher curvature radius of the isosurface of the electric field in the critical region. This might be seen

from the fact that for higher distances W. the breakdown process starts for higher bias voltage than the computed values.
From simulation results it is also seen that for W* more than 400 microns, the breakdown voltage is not influenced by the distance between p+ implant and the cut

ACKNOWLEDGMENTS

We are deeply obliged to CMS Silicon Tracker Group from INFN-Pisa, Italy especially to Prof. G.Tonelli from University of Pisa. for interesting discussions, technical and financial support.

THE AUTHORS

Prof. Dr. Tatiana Angelescu is with the University of Bucharest, Faculty of Physics, Bucharest-Magurele
e-mail:angt@scut.fizica.unibuc.ro

Prof. Dr. Doc. Alexandru Mihul is with the University of Bucharest, Faculty of Physics, Bucharest-Magurele
e-mail: Alexandru.Mihul@cern.ch

Otilia Militaru, Ph.D. student at University of Bucharest, researcher at National Institute of Nuclear Physics and Engineering, P.O box MG-6, 76900 Bucharest-Magurele
e-mail: Otilia.Militaru@cern.ch

Dr. M. Pentia, senior researcher at National Institute of Nuclear Physics and Engineering, P.O box MG-6, 76900 Bucharest-Magurele,
e-mail: Mircea.Pentia@cern.ch

REFERENCES

[1] G. Tonelli, Nucl. Instr. and Meth. A386 (1997) 129-137.
[2] G. Tonelli & al., Nucl. Instr. and Meth. A37 (1996) 422-428.
[3] M. Da Rold & al., Radiation Effects on Breakdown Characteristics of Multiguarded Devices, 1996.
[4] A. Chilingarov & al., Nucl. Instr. and Meth. in Phys. Res. A360, (1995).432-437.
[5] B. Jayant Baliga, Modern Power Devices, 2-nd edition, Ed. J. Wiley & Sons.
[6] S. M. Sze, Semiconductor Devices, Physics and Technology, 3-rd edition, Ed. J.Wiley & Sons.
[7] DESSIS.ISE,, Reference Manual, Vol.3, Integrated Systems Engineering AG, ETH-Zentrum, ETZ, Switzerland.
[8] L. Evensen & al., Nucl. Instr.and Meth. A337 (1993) 44-52.
[9] A. Bischoff & al., Nucl. Instr. and Meth. A326 (1993) 27-37.
[10] M. Laakso & al., Nucl. Instr. and Meth A327 (1993) 517-522.
[11] D. Bisello & al., Il Nuovo Cimento, Vol 109A, N9, September 1996.
[12] N. Bacchetta & al., High voltage operation of silicon devices for LHC experiments, The 7-th Pisa Meeting of Advanced Detectors, La Biodola, Elba, May 1997.
[13] N. Bacchetta & al., Study of Breakdown effects in silicon multi-guarded structures; IEEE Nuclear Symposium and Medical Imaging, 9-15 November 1997, New Mexico.